Acta Montanistica Slovaca
ISSN 1335-1788
actamont.tuke.sk

Study of a Calcium-Containing Inhibitive Water-Based Drilling Fluid with Starch and Biopolymer Additives for Maintaining Wellbore Wall Stability

Tanyana IVANOVA[1], *Aleksandr KORSHUNOV*[*2] *and Vladimir KORETSKII*[3]

Authors' affiliations and addresses:
[1] Udmurt Federal Research Center of the Ural Branch of the Russian Academy of Sciences, Institute of Mechanics, 426000, T. Baramzinoy str., 34, Izhevsk, Russia
e-mail: atatnic2013@yandex.ru,

[2] Udmurt Federal Research Center of the Ural Branch of the Russian Academy of Sciences, Institute of Mechanics, 426000, T. Baramzinoy str., 34, Izhevsk, Russia
e-mail: bmaguser_kai@mail.ru

[3] MIREA - Russian Technological University, 119454, Vernadsky Avenue, 78, Moscow, Russia
e-mail: koretskij@mirea.ru

***Correspondence:**
Aleksandr Korshunov, Udmurt Federal Research Center of the Ural Branch of the Russian Academy of Sciences, Institute of Mechanics, 426000, T. Baramzinoy str., 34, Izhevsk, Russia
tel.: +79128515381
e-mail: kai@udman.ru

How to cite this article:
Ivanova, T., Korshunov, A. and Koretskii, V. (2026). Study of a Calcium-Containing Inhibitive Water-Based Drilling Fluid with Starch and Biopolymer Additives for Maintaining Wellbore Wall Stability. *Acta Monstanistica Slovaca,* Volume 31 (1), 137-146

DOI:
https://doi.org/10.46544/AMS.v31i1.11

Abstract
When drilling tools cut into rock, the stress state of the rock changes, leading to the potential for rockfalls, borehole narrowing, cavity formation, and adhesion. Modeling the distribution of shear and compressive stresses in rock indicates that the most significant rock fractures occur at boundaries between areas of reduced and elevated pressure, or along boundaries of high-pressure zones. To ensure borehole stability and prevent brittle rock failure, a condition is proposed for any point on the borehole wall that allows adjustment of pressure level and drilling fluid density limits. The lower limit represents the minimum required fluid density to prevent wellbore collapse and to ensure resistance to spalling, determined from shear and normal stresses. The upper limit represents the density of the drilling fluid that prevents the formation of fractures and fluid loss into the formation. Field tests have enabled the recommendation of a mineralized starch-biopolymer inhibitive drilling fluid for drilling in complex geological conditions at depths of 1330–1478 m.

Keywords
rocks, rock formations, stresses, fluid density, inhibitors

Introduction

Rocks are classified as multiphase dispersed systems: coarse-dispersed, fine-dispersed, and colloidal (Wang et al., 2024, Yu et al., 2024, Seňová et al., 2023, Majko et al., 2022). Minerals undergoing chemical alterations are more dispersed (e.g., clay rocks), while those with no chemical changes are the most stable and strong (quartz, feldspar). Clay-rich rocks, due to their high hydrophilicity, bind and retain liquids and gases (fluids) within their volume; however, due to the shape of their particles (plate- or needle-like), they exhibit different effects on specific surface area and cohesion. Contact of clay-rich rocks with water alters strength, plasticity, swelling, and stickiness. High rock moisture content reduces gelation, coalescence, adhesion, and coagulation, while increasing absorptive and adsorptive capacity (Liu et al., 2024; Zhu et al., 2023).

The mechanical properties of rocks include compressibility, shear strength, and water permeability (Bembenek et al., 2024, Bołoz et al., 2023, Biały et al., 2024, Biały et al., 2026). Compressibility under external load changes porosity and depends on the compressibility factor and deformation. Compressive deformation of rocks occurs according to the following scheme: mutual displacement of particles into denser packing → fracture of particles and their large aggregates → removal of water and air from rock pores → deformation of water films at contact points → compression of air in closed pores → elastic deformation of mineral particles.

Shear strains induce shear stresses in the rock mass; exceeding the rock's strength causes failure. Shear always occurs along slip surfaces, the orientation and shape of which are determined by rock strength and its ability to resist failure through friction and adhesion (Kelemenova et al., 2020).

The penetration of drilling bit cutting elements into rock via vertical axial feed and rotary motion fractures the bottomhole rock through the following mechanisms: (1) cutting, (2) spalling and crushing, and (3) abrasion (Figure 1). When cutting, a blade or diamond drilling bit experiences a continuous static axial load. Blade and roller cone bits spall or crush rock, causing impacts and additional dynamic loads. A diamond bit fractures the rock through abrasion. The penetration of any bit alters the stress state of the monolithic rock, leading to its instability. The cylindrical wall of the well loses its shape and dimensions; rock pieces collapse, constrictions or cavities appear; wet rock pieces stick to the metal of the drilling tool and, under the pressure of the drilling fluid, form seals, sticking to the tool and the bottom-hole assembly components, causing a slurry plug, adhesion, and differential sticking, which sharply reduce drilling rate, lead to stuck pipe, tool failure, and increased time for remediation (Neskromnykh et al., 2020, Ivanova, 2022, Ivanova et al., 2022a).

In circulating fluid drilling, borehole wall stability at depths below 30 m is ensured by a difference of 2.1–3.0 m (0.21–0.30 bar) between the hydrostatic pressure of the drilling fluid column and the groundwater level (Ivanova et al., 2022a, Ivanova & Zasadzien, 2021, Krenicky et al., 2025). The deeper the groundwater table below the surface—i.e., with increasing drilling depth—the higher the excess hydrostatic pressure required to maintain borehole wall stability. However, in this case, there is a high risk of losses (seepage) of the drilling fluid into the rock pores (Domanski et al., 2017) .

Wellbore stability in complex geological conditions is enhanced by selecting the type and adjusting the parameters of water-based drilling fluid, controlling salinity and cation levels, controlling filtration, and controlling pH (Ivanova & Zasadzien, 2021, Ivanova & Safronov, 2019, Sapronov et al., 2025). Potassium Potassium chloride solutions with filtration rates up to 15 cm^3/30 min and fluid densities matching the abnormally high pore pressure gradient are used when drilling highly hydrated, swelling, clay-rich rocks. For drilling fractured shales in tectonically disturbed zones with steep dip angles, a non-dispersed KCl-based drilling fluid may be used, formulated with polyacrylamide and xanthan gum biopolymer (KK Robus grade, XC polymer type) to maintain an API fluid loss of ≤5 cm^3/30 min.

Polymer-clay fresh and inhibitive types of fluids (Na, Mg, Al, Fe, and their combinations) are applied when drilling moderately hydrated clays (argillites, shales with montmorillonite) with filtration up to 5 cm^3/30 min; they reduce clay swelling in combination with resistance to hydration of clay shales (Ivanova & Safronov, 2019, Ivanova & Gavrilov, 2022, Makarov & Ivanova, 2023). Increasing the stability of the wellbore in sloughing formations is achieved by using silicate fluids, which exchange sodium cations from liquid glass with calcium cations from clay-bearing rocks. The reaction forms insoluble calcium silicate, which acts as a cementing agent (Ivanova et al., 2023, Chizhik et al., 2022, Zhuravkov et al., 2023). Therefore, the study of rock strength under load during well drilling and the determination of well wall stability under the influence of drilling mud using geomechanical approaches are relevant tasks for ensuring the required drilling technology.

Materials and Methods

The objective of this research is to study rock fracture stresses during drilling and to develop a drilling fluid formulation to enhance borehole stability in challenging geological conditions. Furthermore, important components included identifying the relationship between deformation and pressure versus strain rate in clay rocks, modeling residual rock stresses during bit penetration that account for changes in drilling fluid pressure, and improving borehole wall stability using drilling fluid inhibitors.

In general, bit penetration alters in-situ rock stress and induces rock deformation (Figure 1). At the initial stage, the pressure and deformation are directly proportional according to Hooke's law of elasticity (section 1, Figure 1). The stresses remain below the rock strength. With increasing pressure (load), rock compaction occurs; the stresses exceed the resistance limit of the rock particles' structural bonds, gradually shearing them, shifting them, and developing intensive deformation. Section 2 (Figure 1) becomes curvilinear. If the load exceeds the pressure p_2, shear stresses induce slip and rock failure (section 3, Figure 1). A change in the strain rate alters the slope of the strain-pressure curve: line a–b_1 corresponds to low loads, small deformations, and strain rates; line a–b_2 – corresponds to increasing strain rate; line a–b – corresponds to a constant strain rate.

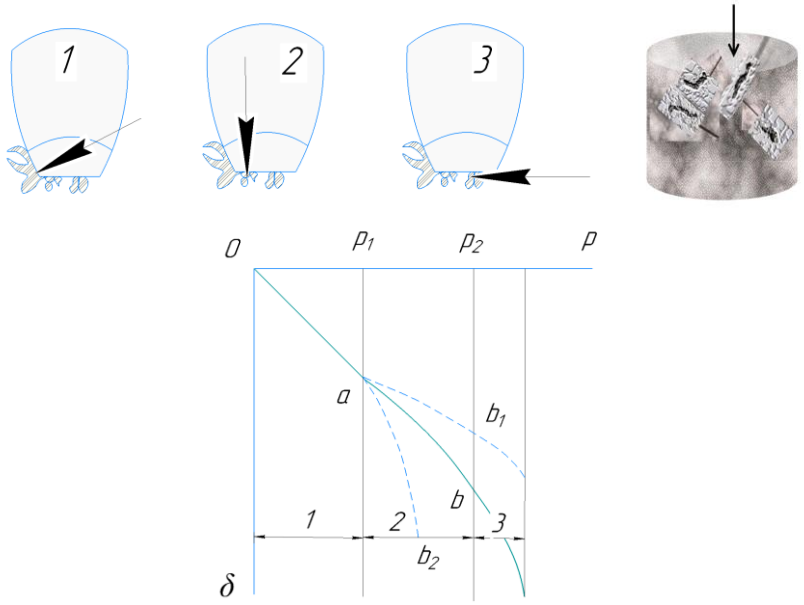

Figure 1. Load action mechanism (1 – cutting, 2 – spalling/crushing, 3 – abrasion), fracture formation mechanism, dependence of rock deformation δ on ambient pressure p

The stronger the interparticle forces, the greater the structural bond cohesion and rock strength. Rock strength factors are determined from ultimate loads that cause failure. The ultimate shear resistance of rock is taken as the shear stress at the loading stage at which shear deformation development ceases (Adigamov & Yudenkov, 2021., Handrik et al., 2016).

In a one-dimensional shear plane, the strength of a rock depends on the ratio of normal compressive stress σ and shear stress τ: the higher the vertical compressive load on the rock, the greater the shear stress required to shear it. The limit equilibrium equation is a straight line offset along the vertical axis τ by the cohesion value c:

$$\tau = \sigma \cdot tg\varphi + c \qquad (1)$$

where φ is the coefficient of internal friction; c is the cohesion (MPa).

Under a triaxial stress state, the strength of the rock depends on the ratio of the principal normal stresses $\sigma_1, \sigma_2, \sigma_3$ and the shear stress τ, determined graphically by the Mohr-Coulomb circles with radii of the great circle $r_б = 0{,}44 \cdot (\sigma_1 - \sigma_3)$, a small circle $r_м = 0{,}5 \cdot (\sigma_2 - \sigma_3)$ with the center at the point $(0{,}5 \cdot (\sigma_2 + \sigma_3), 0)$; a medium circle $r_c = 0{,}5 \cdot (\sigma_1 - \sigma_2)$ with the center at the point $(0{,}5 \cdot (\sigma_1 + \sigma_2), 0)$. The total pressure, replacing the action of the forces of cohesion and friction, is determined by the formula

$$P = c \cdot ctg\varphi.$$

On the graph this is point A, from which the limit tangent to the circles AB is drawn, characterizing the parameters of the rock shear strength c and φ (Figure 2).

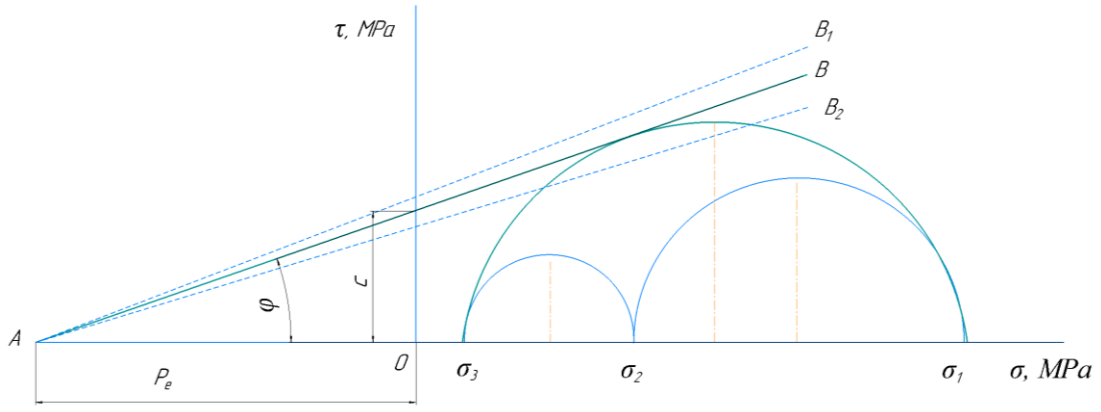

Figure 2 - Mohr-Coulomb stress circles

Cohesionless rocks (sand, loamy sand) exhibit shear strength without cohesion but with internal friction. The shape and surface characteristics of the particles determine the shear strength of such rocks. Rounded rock particles reduce the angle of internal friction (φ) by reducing frictional forces and particle interlocking. Angular particles with an uneven rough surface increase the angle of internal friction (φ), cohesion, and frictional forces between particles. With increasing dispersion, the angle of internal friction (φ) and particle cohesion decrease. Compared to dense rocks, unconsolidated and loose rocks have higher porosity and a smaller angle of internal friction. Fluid presence in cohesionless rocks reduces interparticle friction and the angle of internal friction. The shear resistance of cohesive rocks (loam, clay) is characterized by cohesion that varies widely and a high friction coefficient. In rocks with an oriented texture, shear along the direction of particle orientation occurs more easily than across their orientation. With increasing moisture content of cohesive rocks, the cohesion (c) and the angle of internal friction (φ) decrease due to the weakening of structural bonds and the lubricating action of the drilling fluid.

Exceeding the Mohr-Coulomb boundary state of stress (line AB_1, Figure 2) causes irreversible fracture deformation in rock. Reducing the Mohr-Coulomb boundary state of stress below the ultimate load reduces fracture density and extent in the rock, making it stronger (line AB_2, Figure 2).

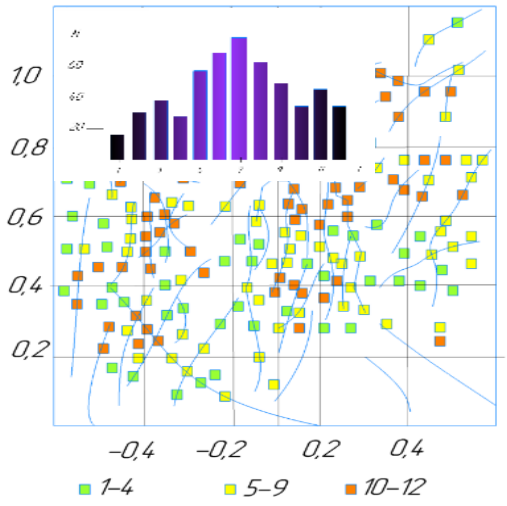

Figure 3 - Parameters determining stresses at rock formation calculation nodes. The vertical axis is the formation thickness (meters); the horizontal axis is the borehole deviation from the vertical (degrees). Diagram data: I is the number of calculation iterations determining the sample N. The legend (lower axis) is the number of calculations at the points

Fracture modeling was performed with Rosneft software suites (Guluzade, 2022). When analyzing rupturing deformations, an algorithm for generating homogeneous samples with an identical averaging scale, depending on the fracture distribution density and the homogeneity of their propagation kinematics, was considered. Modeling results of stresses at each calculation node enable monitoring of stress state for a specific well and by reservoir thickness (Figure 3). Most of the studied wells are characterized by a state of deformation in the form of vertical shear, with local zones of horizontal compression and areas of horizontal tension. In this

case, a state close to pure shear (from –0.2 to +0.2 degrees of deviation from the vertical axis of the well per 1 m of length) corresponds to 68–70% of the points.

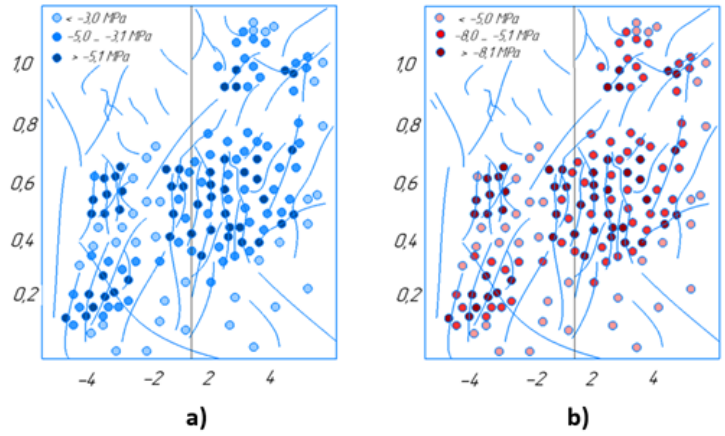

Figure 4 - Distribution of minimum (a) shear stresses and maximum (b) compressive stresses in rock modeling. The vertical axis is the formation thickness (meters); the horizontal axis is the borehole deviation from the vertical (degrees). The legend shows the normalized stress ratio σ/τ.

Stress modeling results show that maximum shear stresses exceeding 35 MPa are distributed over an area of 30–35% and exceed the cohesion strength of rock by 4–6 times. Reduced stress levels below 10 MPa are distributed in the zone of branched fractures and constitute 10% of the total area, with a strength 2–3 times exceeding rock cohesion; zones of minimal fracture propagation occupy 50–60% of the total area with strength equal to rock cohesion. High pressure exceeds the cohesion strength by 8–10 times over an area of no more than 15%, while low-pressure forces, 3–4 times lower than the cohesion strength, occupy areas of no more than 5–7% of the total area. The largest rock fractures occur at the boundaries between areas of reduced and elevated pressure, and along the boundaries of areas with high pressure. Analysis shows that it is possible to vary stresses and pressures. For example, maximum shear stress increases by 0.8τ for a 0.5τ increase in pressure, as confirmed in practice. A relationship has been identified whereby compressive stress in rock depends on shear stresses: the maximum value $\sigma = 0.85\tau$ and minimum value is 0.6τ. The model accuracy was experimentally confirmed via downhole measurements.

To ensure the stability of the borehole walls and prevent the occurrence of brittle fracture of rocks, drilling fluid pressure p_q can be adjusted so that at any wellbore wall point, the following condition holds:

$$\tau + (\sigma - p_q)tg\varphi \leq \sigma \cdot tg\varphi + c \qquad (2)$$

Adjusting drilling fluid pressure by setting a fluid density limit can ensure the strength and stability of borehole walls against brittle shear fractures and fracture formation. The lower limit is the minimum required drilling fluid density to prevent borehole wall collapse and spalling. The upper limit corresponds to the fluid density that prevents the formation of an open fracture and fluid loss into the formation. The lower limit corresponds to the left-hand side of condition (2) and is related to the definition of σ_3 or σ, while the upper limit represents the right-hand side of condition (2), responsible for tensile fracture formation. Drilling fluid density is calculated based on the hydrostatic pressure exerted by the fluid column at the bottomhole when exposing a producing horizon, with the calculated density exceeding the design value by no more than 5–10%.

The formulas for the ultimate stress limits at any point in the rock massif under the bit are distributed as shown in Figure 5 and according to the following formula:

$$\sigma_1 = \frac{P}{\pi}(2b + sin\ 2b),\ \sigma_2 = \frac{P}{\pi}(2b - sin\ 2b) \qquad (3)$$

where b is the width of the bit cutters, P is the total pressure replacing the action of cohesion and friction forces.

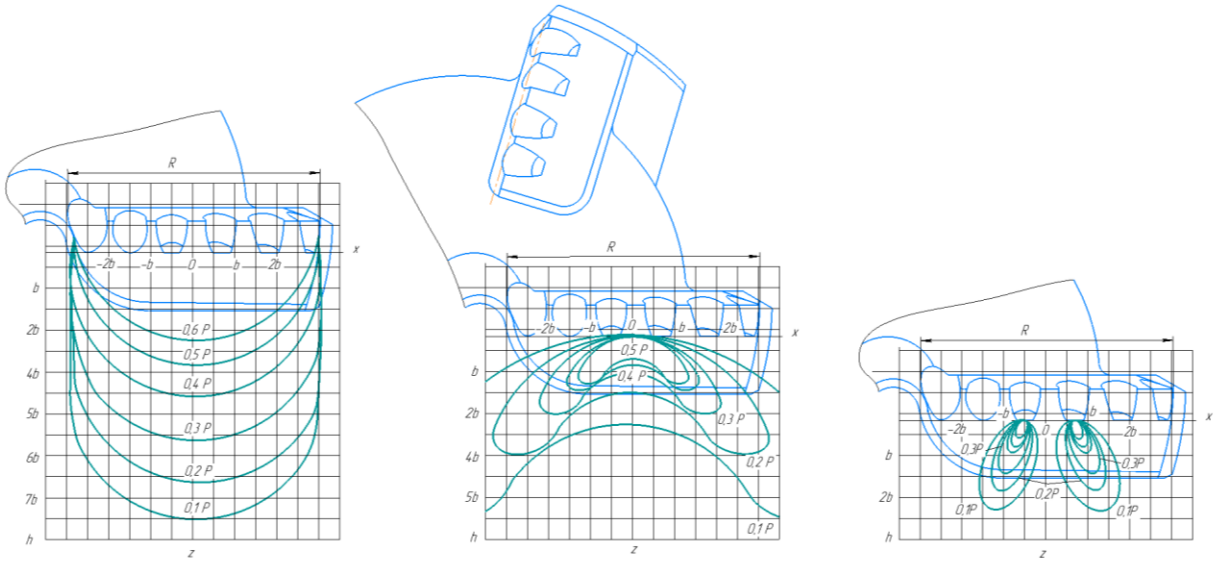

Figure 5 - Distribution of vertical compressive normal stresses (a), horizontal normal tensions (b), and shear stresses causing slips (c)

The influence of vertical stresses σ with an intensity of 0.1P extends to a depth of 7.5b (Figure 5a), while horizontal tensions and tangential stresses are distributed at the same intensity at a depth of 5.3b and 2.3b (Figure 5b, c).

The penetration radius of the bit-cutting elements affects the depth of stress propagation. Due to rotation about its axis, vertical feed, the static and dynamic effects of the drilling tool, and rock strength, not all drilling bit roller cone cutters are engaged in the work at the same time. One tooth may penetrate, while others cut, abrade, wear, crush, or spall; thus, the stress distribution is unique for each cutter. However, the overall cumulative effect of a single bit cutter—for example, from vertical stresses—is equalized overall along the radius of the bit cutting elements (Figure 5a) to a depth of no more than 7b. Similarly, horizontal normal tensions and shear stresses act collectively from each cutter (Figure 5b and 5c). In the absence of anomalous geological conditions, adjusting density, pressure, and force reduces the ultimate stresses and ensures borehole wall stability, but only at shallow depths.

Instability during drilling of clays and clay-rich rocks occurs due to abnormally high pore pressure, bulk density, porosity, moisture content, and pore-water salinity. When drilling highly swelling clays (montmorillonite), a pH of 6–7 is recommended; for medium swelling clays, a pH of 6–9; and for weakly swelling clays, a pH of 8–9, respectively. The moisture content of the clay-rich rock should be less than 5%. Clay semi-permeability is characterized by its charge and the presence of a double electric layer. Negatively charged OH^- anions and cations penetrate the clay, transporting fluid. Experiments show that in H_2O, clay disintegrates within 11 hours; in H_2O + NaOH and H_2O + 10% NaCl solutions, disintegration occurs after 2.5 and 6 hours, respectively; with H_2O + 10% KCl, it does not disintegrate even after 102 hours. The increase in the time to clay non-disintegration is due to potassium ion mobility in KCl, which neutralizes the negative charges on the anions and clay, leading to rock stability. NaCl is added to simulate natural fluid salinity, which stabilizes the borehole walls, fixes sodium ions at cation-exchange sites in clay minerals, and converts them into a more stable, non-swelling form. If drilling fluid salinity exceeds that of pore water, water flow from the formation to the wellbore increases clay rock stability.

To determine the stability conditions, experimental and field studies were conducted at the deposit to determine and interpret the mechanical rock properties with inhibitor introduction.

In laboratory tests, drill-cutting samples of equal mass, pre-pressed and dried, were subjected to a 4-hour exposure in two fluids: drilling fluid 1 (sample 1) and fluid 2 (sample 2). The drilling fluid components are presented in Table 1.

The results showed the following outcomes. Sample 1 became soft after 4 hours and lost its shape, disintegrated when transferred to the scales, adhered to any surface, and crumbled when a slight force was applied (Fig. 6, sample 1) (Pivarciova et al., 2019). Sample 2, after 4 hours, became moderately soft, retained its shape and structure, showed no fragmentation after transfer to the scales; when a force of up to 82 dPa was applied, sample 2 retained its structure and shape, but when a force of 85 dPa was applied, it crumbled (Fig. 6, sample 2). Sample 2 demonstrates pronounced inhibitive properties of fluid 2; the clay is less susceptible to swelling, with no mass increase.

Table 1. Type and parameters of drilling fluidsJZ

Interval (along borehole), m		Drilling fluid components	Fluid density, g/cm^3	pH	Filtration, cm^3 /30 min	Concentration of colloidal phase MBT kg/m^3	Apparent viscosity AV ft/100 ft^2	Dynamic shear stress (DSS), daPa	Funnel viscosity FV, sec	Conventional proof stress, kPa
from	to									
250	1000	Basic fluid: Clay 5 – 10%; Polymer – 2%; Na_2CO_3 – 0.03%	1.15	10	20	71.25	5.5	62-95	60	93
253	530 - 585	Fluid 1: Naturally occurring chemically treated clay suspension; KSSB-2M; Defoamer; Soda ash (Na_2CO_3) – 3%; Clay inhibitor: GKZh-11 – hydrophobizing organosilicon liquid CMC-800 – sodium carboxymethylcellulose - Lost circulation material – filler	1.10-1.15	10.5	146	45.75	2.0	81.6	61-84	110
1213	1330-1478	Fluid 2: Salted starch-biopolymer drilling fluid Defoamer – 4% Starch reagent – 10% Xanthan biopolymer – 5% Lubricating additive – 1% Clay inhibitor: calcium carbonate – 20% or not less than 800 mg/l Bactericide – 1% Natural ground chalk (marble grit) – 3%	1.15	9	66	57	1.0	80-120	42-54	150

Sample 1

Sample 2

Figure 6 – Drill cutting samples after tests

Results

Carboxymethyl cellulose (CMC polymer) forms a thin filter cake on the borehole wall and around drill cutting particles. On the borehole walls, the cake prevents drilling fluid penetration into the water-bearing porous formations. In drilled clay-rich formations, the cake prevents solution absorption, swelling, and narrowing of the borehole cross-section. When drilling through clay, the cake prevents the clay from disintegrating into the finest particles that would contaminate the circulating fluid. Clay lumps are preserved and settle in the surface pits. CMC products protect the aquifer, improving the removal and sedimentation of drilled clay particles. They also increase the viscosity of the drilling fluid to some extent. CMC forms a cake that consolidates the borehole walls and enables the clay cuttings to be removed. For cohesive soils (clays), CMC is used at a rate of 8 kg/m³.

Bentonites are activated clay powders that increase the viscosity of drilling fluid and, through gelling, stabilize large soil particles, thereby stabilizing wellbore walls. However, high concentrations impair the sedimentation of drill cuttings in the surface pits.

Wellbore wall stabilization depends on the difference between the groundwater level and the circulating drilling fluid level. If the difference is large and the groundwater is deep enough, the drilling fluid can infiltrate the aquifer at high pressure, resulting in total losses. If the groundwater table in an artesian aquifer lies above the

static groundwater table, adding weighting agents creates a sufficiently high backpressure in the drilling column. Additionally, the drilling fluid level must not drop below the groundwater table; otherwise, the well collapses. In this case, wellbore protection can be achieved by creating a thick filter cake, i.e., by adding carboxymethyl cellulose, if the groundwater table cannot be adjusted.

The test results for the corresponding drilling fluids (Solutions 1 and 2) are presented in Table 1. In complex geological conditions, the fluids showed reduced colloidal-phase MBT concentration, apparent viscosity (AV), and yield point (YP), and significantly higher filtration than the base fluid. Inhibitive clay-based drilling fluids (Fluids 1 and 2) exhibited lower colloidal phase content than the base fluid. Fluid 2 carries calcium and sodium ions, which positively affect the inhibitory effect (Elbakian et al., 2018). A starch reagent is necessary to reduce filtration, which positively affects the conditional ultimate shear strength and the stability of the borehole walls. Fluid 2 is neutral to formation saline water, shows no coagulation, and formation cuttings do not affect fluid properties. Fluid 1 demonstrated lower inhibition capacity than Fluid 2; increased filtration and funnel viscosity resulted from exposure to formation acidic waters and anhydrites. However, this fluid is simple to prepare and environmentally safe. For drilling clay formations in complex geological conditions, Fluid 2 was recommended.

Conclusions

Research revealed that the rate of the deformation–pressure curve depends on strain rate: the curve lies above the directly proportional line corresponding to low loads, small deformation, and strain rate; the curve lies below the directly proportional line with significant strain rate increase; the directly proportional line is observed at constant strain rate.

Rock strength parameters were determined at ultimate loads causing failure. Ultimate rock shear resistance is taken as the shear stress at the loading stage at which shear deformation development ceases. It was established that cohesionless (loose) rocks (sand, loamy sand) exhibit no cohesion under shear but possess internal friction; rock strength depends on particle shape, surface character, and fluid presence. A feature of cohesive rock (silty clay, clay) shear resistance is the presence of cohesion and a high friction coefficient. With increasing moisture content in cohesive rocks, cohesion and the internal friction angle decrease due to weakened structural bonds and the lubricating action of the drilling fluid. Exceeding ultimate stress state values causes irreversible fracture deformations in rock. Reducing ultimate stress state values below the ultimate load level decreases the quantity and extent of fractures, making the rock stronger.

Stress modeling results at each calculation node enable monitoring of the stress state for a specific well and formation thickness. Most of the studied wells are characterized by a deformation stress state in the form of vertical shear, with local zones of horizontal compression and horizontal tension. Modeling of minimum shear stress and maximum compressive stress distributions in rock showed that the largest rock fractures occur at boundaries between zones of reduced and elevated pressure, and along boundaries of high-pressure zones.

To ensure wellbore wall stability and prevent brittle rock failure, a condition is proposed for any wellbore wall point, allowing adjustment of pressure level and drilling fluid density limits. The lower limit represents the minimum required fluid density to prevent wellbore collapse and ensure resistance to spalling, determined by shear and normal stresses; the upper limit represents the fluid density that prevents open fracture formation and fluid loss into the formation. Field trials enabled the recommendation of a mineralized starch-biopolymer inhibitive drilling fluid for drilling at depths of 1330–1478 m in complex geological conditions.

References

Adigamov, A.E. and Yudenkov, A.V. (2021). Stress–strain behavior model of disturbed rock mass with regard to anisotropy and discontinuities. Mining Informational and Analytical Bulletin, (8), 93–103.

Bembenek, M., Grydzhuk, Y., Gajdzik, B., Ropyak, L., Pashechko, M. and Slabyi, O. et al. (2024). An analytical–numerical model for determining drill string–wellbore frictional interaction forces. Energies, 17(2), 301.

Biały, W., Prostański, D. & Bołoz, Ł. (2024) „Selection of longwall shearers based on the results of research on the mechanical properties of coal". Scientific Reports 14, 18606. https://doi.org/10.1038/s41598-024-69178-w pp. 1-11

Biały, W., Szkudlarek, Z., Szweda, S., Bernatt, J., & Turczyński, K. (2026). Stand Tests of Energy Consumption While Rock Mining with the Use of Experimental Cutterhead Tilt Angle. Applied Sciences, 16(3), 1605. https://doi.org/10.3390/app16031605

Bołoz Ł., Biały W. (2023) „Methods and Test Benches for Cutting Tools Testing – A Review". Energies, 16, 445. https://doi.org/10.3390/en16010445

Domanski, T., Sapietová, A., Sága, M. (2017). Application of Abaqus software for the modeling of surface progressive hardening. XXI POLISH-SLOVAK SCIENTIFIC CONFERENCE MACHINE MODELING AND SIMULATIONS MMS 2016, Vol. 177, Page 64-69, DOI10.1016/j.proeng.2017.02.184

Elbakian, A., Sentyakov, B., Bozek, P., Kuric, I., Sentyakov, K. (2018). Automated separation of basalt fiber and other earth resources by the means of acoustic vibrations. In Acta Montanistica Slovaca. Vol. 23, no. 3 (2018), pp. 271-281.

Guluzade, T.E. (2022). Study the membrane efficiency while drilling clay rocks. Azerbaijan Oil Industry Journal, (1), 16–20.

Handrik, M., Kopas, P., Baniari, V., Vasko, M., Saga, M. (2016). Analysis of stress and strain of fatigue specimens localised in the cross-sectional area of the gauge section testing on bi-axial fatigue machine loaded in the high-cycle fatigue region. XXI POLISH-SLOVAK SCIENTIFIC CONFERENCE MACHINE MODELING AND SIMULATIONS MMS 2016, Vol. 177, Page 516-519, DOI10.1016/j.proeng.2017.02.254

Chizhik, S.A., Zhuravkov, M.A., Petrovskiy, A.B. and Prushak, V.Y. (2022). Calculation of the effective mechanical characteristics of the undermined rock mass. Doklady National Academy of Sciences of Belarus, 66(1), 83–90.

Ivanova, T.N. (2022). Mining and geological features of well drilling in Western Siberia. Aspects in Mining & Mineral Science, 9(4), 717.

Ivanova, T.N. and Gavrilov, K.N. (2022). Application of clay drilling mud with polymer reagent. Scientific Engineering Technologies (Polytech Bulletin), (3), 112–114.

Ivanova, T.N. and Safronov, S.I. (2019). Drilling fluids used in the fields of the Udmurt Republic. In: Savenok, O.V. (ed.) Readings of A.I. Bulatov: Materials of the III International Scientific and Practical Conference. Krasnodar: Yug Publishing House, pp. 64–67.

Ivanova, T.N. and Zasadzien, M. (2021). Technological capabilities of well cementing. Multidisciplinary Aspects of Production Engineering, 4(1), 465–478.

Ivanova, T.N., Korshunov, A.I. and Abo Issa, N. (2022). Technology of drilling of slant well on the field of Western Siberia. Acta Montanistica Slovaca, 27(2), 417–429.

Ivanova, T.N., Krenicky, T., Korshunov, A.I. and Koretskii, V.P. (2023). Water production isolation techniques for oil-wells with high reservoir temperature. MM Science Journal, 2023(2), 1042–1054.

Kelemenová, T., Dovica, M., Bozek, P., Koláriková, I., Benedik, O., Virgala, I., Prada, E., Miková, Ľ., Kot, T., Kelemen, M. (2020). Specific Problems in Measurement of Coefficient of Friction Using Variable Incidence Tribometer. In Symmetry. Vol. 12, iss. 8 (2020), pp. 1-20. DOI: 10.3390/sym12081235

Krenicky T., Dyadyura K., Kokhan O., Umynskyi S. (2025) Modelling the heat and mass transfer in devices with dense-layer dispersed systems. Management Systems in Production Engineering 2025 Volume 33, Issue 4, pp. 470-477 DOI 10.2478/mspe-2025-0046

Kuric, I., Klarak, J., Bulej, V., Saga, M., Kandera, M., Hajducik, A., Tucki, K. (2022). Approach to Automated Visual Inspection of Objects Based on Artificial Intelligence. APPLIED SCIENCES-BASEL, Vol. 2I, Issue 2, DOI10.3390/app12020864

Liu, Y., Bai, J., Guo, P., Zhang, W., Zhong, L. and Lyu, C. et al. (2024). Experimental study on water-in-heavy-oil droplets stability and viscosity variations in the dilution process of water-in-heavy-oil emulsions by light crude oil. Energies, 17(2), 332.

Majko, J., Vasko, M., Handrik, M., Saga, M. (2022). Tensile Properties of Additively Manufactured Thermoplastic Composites Reinforced with Chopped Carbon Fibre. MATERIALS, Vol. 15, Issue 12, DOI10.3390/ma15124224

Makarov, M.K. and Ivanova, T.N. (2023). Technologies for blocking zones of drilling fluid absorption by local well casing equipment. Technosphere Management, 6(1), 1–10.

Neskromnykh, V.V., Popova, M.S., Golovchenko, A.E., Petenev, P.G. and Baochang, L. (2020). Method of drilling process control and experimental studies of resistance forces during bits drilling with PDC cutters. Journal of Mining Institute, 245, 539–546.

Pivarciová, E., Domnina, K. and Ságová, Z. (2019). Design of the construction and research of vibrations and heat transfer of mine workings. Acta montanistica Slovaca 2019 24 (1), pp. 15-24

Sága, M., Bednár, R. Vasko, M. (2011). Contribution to Modal and Spectral Interval Finite Element Analysis. VIBRATION PROBLEMS ICOVP 2011, Vol. 139, Page 269-274, DOI10.1007/978-94-007-2069-5_37

Sapronov O., Buketov A., Sapronova L., Mokiy O., Vorobiov P., Banha M., Straka L. (2025) Improvement of thermophysical characteristics of polymer coatings for protecting water transport by using a mixture of discrete organic fibers. Management Systems in Production Engineering Volume 33, Issue 4, pp. 576-585 DOI 10.2478/mspe-2025-0060

Seňová A., Pavolová H., Škvareková E. (2023) Assessment of the impact of working risks in the exploitation of raw materials. Management Systems in Production Engineering. Volume 31, Issue 1. pp. 86-94. doi: 10.2478/mspe-2023-0011

Wang, F., Li, B., Cao, S., Zhang, J., Xu, Q. and Sang, Q. (2024). Experimental study of the fluid contents and organic/inorganic hydrocarbon saturations, porosities, and permeabilities of clay-rich shale. Energies, 17(2), 524.

Yu, Y., Shen, K. and Zhao, H. (2024). Experimental investigation of fracture propagation in clayey silt hydrate-bearing sediments. Energies, 17(2), 528.

Zhu, P.F., Zhang, H., Pivarciová, E., Sfarra, S., Maldague, X. (2023). Characterization of water content and inspection of delamination in spruce, oak and meranti woods after pyrolysis processing using a new terahertz time-domain spectroscopy method. NDT & E INTERNATIONAL, Vol. 139, Published Oct. 2023, DOI10.1016/j.ndteint.2023.102938

Zhuravkov, M.A., Petrovskiy, A.B., Prushak, V.Y. and Chizhik, S.A. (2023). Modeling of the geomechanical state of the rock massifs being undermined repeatedly. Proceedings of the National Academy of Sciences of Belarus. Physics-Technical Series, 68(1), 32–39.